NUMERICAL STUDY OF CELLS MOLECULAR UPTAKE DUE TO ELECTROPORATION BY USING DIFFERENT SHAPES OF HIGH VOLTAGE ELECTRIC PULSES

D. Miklavcic[1], L. Towhidi[2]
[1] University of Ljubljana, Faculty of Electrical Engineering, Ljubljana, Slovenia, [2] Tarbiat Modares University, Department of Medical Physics, Tehran, Iran.

Corresponding Author: D. Miklavcic, University of Ljubljana, Faculty of Electrical Engineering
Trzaska 25, 1000 Ljubljana, Slovenia; Damijan.Miklavcic@fe.uni-lj.si

Abstract. High voltage electric pulses have been reported to enhance molecular uptake of cells significantly due to formation of transient aqueous pores in the cell membrane. This technique (named electroporation) nowadays is widely used in delivery of a large variety of molecules such as drugs and DNA in biotechnology and medicine. It was experimentally demonstrated that the efficiency of electroporation is under the control of electric pulse parameters. However, the theoretical basis for these experimental results and dependences is theoretically not fully explained. In order to predict the outcome of experiments and optimize the efficiency of electroporation before each treatment, we developed a model by which we investigated the effect of pulse shape on efficiency of electroporation using modelling and simulation. Our model was based on previously developed chemical-kinetics scheme with two types of pores considering membrane conductivity change based on trapezium barrier model while self-consistency was considered. This model was supplemented with a molecular transport model for a single cell to acquire the molecular uptake of cells.
The investigated pulse shapes in our study were unipolar rectangular pulses with different rise and fall time, triangular, sinusoidal and bipolar rectangular pulses and also sinusoidal modulated unipolar pulses with different percentages of modulation. The obtained results from our modelling and simulations are in good agreement with previously published experimental results.

1 Introduction

The cell membrane acts as a barrier that hinders the free entrance of most hydrophilic molecules into the cell. One of the investigated applications of electromagnetic fields which have numerous applications in medicine and biology is the incorporation of impermeate molecules such as macromolecules, drugs and proteins into biological cells without causing any cell physiological malfunctioning. An efficient technique in this respect is electroporation [14],[16],[24],[11]. In electroporation, cells are exposed to a high intensity electric fields (about hundreds V/cm) of short duration (in μs and ms range) in vitro or in vivo. Therefore, permeability of the plasma membrane increases transiently and reversibly for appropriate pulse parameters which result in high enough transmembrane voltage. Because of effective delivery of drugs, proteins and macromolecules, this method is nowadays widely used in biotechnology [3],[25] and in the medical applications such as electrochemotherapy [23],[12], gene electrotransfer, [5], and transdermal drug delivery [18].

It was experimentally demonstrated in several studies that the efficiency of electroporation is under the control of electric pulse parameters such as pulse amplitude, duration, and shape. Optimization of electric field parameters for successful electroporation needs time consuming and costly experiments for different experimental criteria unless an appropriate model for this phenomenon can be suggested. Although several models were proposed in previous studies [2],[6],[7],[8],[13], they are still unable to explain the effect of some parameters such as pulse shape, pulse repetition frequency and number of pulses on uptake enhancement of the cells under exposure.

The suggested mechanism for electroporation is structural changes resulting in formation of transient aqueous pores in the cell membrane. In order to reveal exact mechanisms and dynamics of pore formation and closure and more importantly resealing of membrane theoretical models have drawn great deal of attention.

In our present study, we investigated the effect of pulse shape on efficiency of electroporation using modeling and simulation. Our model was based on chemical-kinetics scheme with two types of pores [15], which has been confirmed recently [1]. We used previously developed equations with field dependent rate coefficients in order to obtain distribution of pores on the membrane. In addition, the conductivity of pores was defined based on trapezium barrier model for the image forces [9]. Self-consistent set of equations were used to consider all simultaneous changes. This model was supplemented with a molecular transport model for a single cell to acquire the molecular uptake of cells. The investigated pulse shapes in this study were unipolar rectangular pulses with different rise and fall time, triangular, sinusoidal and bipolar rectangular pulses and also sinusoidal modulated unipolar pulses with different percentages of modulation.

2 Model Description

2.1 Modified chemical-kinetics model for electroporation

When a cell is exposed to an external electric field, induced transmembrane voltage (ITV) starts to increase based on Laplace equation which leads to structural changes of the cell membrane. Based on previously suggested [15], and recently confirmed [1], model, this structural changes result in two types of pores (chemical-kinetics scheme (1). In this scheme the intact closed lipid state (C) transition to porous state (P2) occurs with two intermediates: One is a tilted lipid head group or intermediate closed state (C1) and the other one is a prepore or transient pore state (P1). The scheme can be described by:

$$C \underset{k_{-1}}{\overset{k_1}{\rightleftharpoons}} C1 \underset{k_{-2}}{\overset{k_2}{\rightleftharpoons}} P1 \underset{k_{-3}}{\overset{k_3}{\rightleftharpoons}} P2 \tag{1}$$

The permeability of P1 state is negligibly small and predominantly P2 is responsible for molecular uptake. Pore formation and closure are denoted by k_i and k_{-i} (i=1,2,3) rate coefficients, respectively. For simplicity, the rate coefficients k_1, k_2 and k_3 are considered equal ($k_1=k_2=k_3=k_p$) [15]. The governed rate laws of constituting steps for the scheme (1) are:

$$\begin{aligned}
\frac{d[C(\vec{r},t)]}{dt} &= -k_p[C(\vec{r},t)] + k_{-1}[C1(\vec{r},t)] \\
\frac{d[C1(\vec{r},t)]}{dt} &= -k_p([C1(\vec{r},t)] - [C(\vec{r},t)]) - k_{-1}[C1(\vec{r},t)] + k_{-2}[P1(\vec{r},t)] \\
\frac{d[P1(\vec{r},t)]}{dt} &= -k_p([P1(\vec{r},t)] - [C1(\vec{r},t)]) - k_{-2}[P1(\vec{r},t)] + k_{-3}[P2(\vec{r},t)] \\
\frac{d[P2(\vec{r},t)]}{dt} &= k_p[P1(\vec{r},t)] - k_{-3}[P2(\vec{r},t)]
\end{aligned} \tag{2}$$

where t and $\vec{r}$ denote time and position, respectively. [C], [C1], [P1] and [P2] show normalized distribution of each membrane lipid state relative to the initial value of closed state $[C(\vec{r},0)]$ [15].

Regarding Van't Hoff relationship in electro-thermodynamics, the rate coefficient of pore formation can be obtained from [15], [9]:

$$k_p = k_{p0} \exp\left(\frac{\Delta V_p \varepsilon_0 (\varepsilon_W - \varepsilon_L)}{2 k_B T d_m{}^2} ITV^2 \right) \tag{3}$$

where ITV is potential difference between the outer and inner layer of the membrane, ΔV_p is the mean volume change due to pore formation, ε_0 is the permittivity of the vacuum and ε_W and ε_L are dielectric constants of water and lipids, respectively. k_B is Boltzmann constant, d_m is the thickness of the membrane and T is temperature. While pore formation rate coefficient k_p is electric field dependent, the closure rate coefficients (k_{-1}, k_{-2} and k_{-3}) are constant and independent of electric field strength [15].

Whenever electroporation occurs, an increase in conductivity during the pulse is observed [17], which can be explained by the formation of pores in the cell membrane. Based on the trapezium barrier model for the image forces [9],[22], the intrinsic pore conductivities $\sigma_{p,i}$ (i=1 and 2 represents P1 and P2 pores respectively) are expressed as follows [9],[22]:

$$\sigma_{p,i} = \sigma^0_{p,i} \exp\left(\alpha_{p,i} n |ITV| \frac{F}{RT} \right) \tag{4}$$

where

$$\sigma^0_{p,i} = \frac{\sigma_{ex} + \sigma_{in}}{2} \exp\left(\frac{-\varphi^0_{im,i} F}{RT} \right) \quad \text{and} \quad \alpha_{p,i} = 1 - \frac{RT}{F \varphi^0_{im,i}} \tag{5}$$

In the above equations, σ_{ex} and σ_{in} are the extracellular and intracellular conductivities respectively, n is the geometrical parameter of the trapezium model for energy barrier, F is Faraday constant and $\varphi^0_{im,i}$ is the intrinsic pore barrier potential.

Therefore conductivity of membrane (σ_m) can be obtained by:

$$\sigma_m(\vec{r},t) = \sigma_{m0} + [P1(\vec{r},t)] \times \sigma_{p,1} + [P2(\vec{r},t)] \times \sigma_{p,2} \tag{6}$$

where σ_{m0} is the physiological/baseline conductivity of membrane. Thus conductivity at each point on the membrane changes with time during and after the pulse depending on pores distributions variations which affect ITV and in turn the distribution of pores.

2.2 Transmembrane molecular transport model

Based on previous studies [4], [26], we defined two distinct phases for electroporated membrane and two related transport mechanisms: the first one is porated phase [P2] with relatively fast relaxation due to pore closure according to Eq. 1. The second phase is memory phase [M] due to enhanced membrane perturbation and ruffling with quite slow relaxation [4],[26], which returns to its baseline value with a dual exponential decay function, [15]:

$$[M] = [P2]_e \left(B \exp(-k_f t) + (1-B) \exp(-k_s t) \right) \tag{7}$$

where $[P2]_e$ is the normalized distribution of [P2] pores at the end of pulse, k_f and k_s are decay rate coefficients for this second phase and B is a constant.

Thus the permeability of the membrane can be written as the sum of two distinct contributions:

$$P_m(\vec{r},t) = \left([P2(\vec{r},t)] D_p / d_m \right) + \left([M(\vec{r},t)] D_r / d_m \right) \tag{8}$$

where D_p and D_r are the diffusion coefficients for interactive transport and endocytotic-like transport, respectively. Due to very short duration of pulses, diffusion is predominant transport mechanism for small molecule uptake [19].

While the membrane is being permeabilized due to electric field, the molecules pass through the membrane due to concentration gradient. A quantitative description of diffusion is contained in the Fick's first law. The total flux can be approximated by $j = P_m(c^{out} - c^{in})$, where c^{out} and c^{in} are the outside and inside concentrations adjacent to the membrane. The total number of molecules transported through the membrane (N) was computed with integration of transported molecules through the cell membrane over the time and the cell surface:

$$N = N_A \int_{t=0}^{\tau} \int_{S} j dS dt \tag{9}$$

where S is the surface of the cell membrane, τ is the time at which the quantity of transported molecules is to be determined and N_A is Avogadro's number.

3 Construction of the model

The simulations in this study were performed using COMSOL 3.3 package (COMSOL Inc., Burlington, MA) based on finite element method. For constructing the geometrical model, a spherical cell with radius of 5.6 μm was located between two virtual electrodes. As incorporating extremely thin membrane is problematic in meshing and solving the problem, we assigned boundary condition to the membrane [20]. We neglected the resting transmembrane voltage. The initial intracellular and extracellular concentrations of probe were set to be 0 and 10 mM, respectively. The diffusion coefficients for interactive diffusion and for induced endocytotic-like process are considered as $D_0/5$ and $D_0/10000$. These two values however depend considerably on the type and size of the transported molecules. The necessary parameters used in our simulations are given in Table 1 [15],[16], [9], [22], [20]. Our simulation was designed to solve the Laplace equation considering all adjoined equations in this model (Eq. (2), (3), (6)) taking into account self consistency of parameters to find the distribution of pores on the cell membrane, spatially and temporally and all related parameters such as ITV, cell membrane conductivity and permeability. Afterwards, the uptake of the cells for each different pulse shapes were obtained. All simulations were performed on a PC (2.8 GHz Pentium IV processor, 3 GB RAM).

The investigated pulse shapes in our study were unipolar rectangular pulses with different rise and fall time of 2, 10 and 100 μs (Figure (1a) to (1c)); triangular, sinusoidal and bipolar rectangular pulses (Figure (1d) to (1f)); and also sinusoidal modulated unipolar pulses with different percentages of modulation of 10% and 90% with 50 kHz frequency (Figure (1g) and (1h)).

Parameter	Symbol	Value
Membrane thickness	d_m	5e-9 m
extracellular conductivity	σ_{ex}	0.14 S/m
intracellular conductivity	σ_{in}	0.3 S/m
initial conductivity of membrane	σ_{m0}	5e-7 S/m
extracellular permittivity	ε_o	7.1e-10 As/Vm
intracellular permittivity	ε_i	7.1e-10 As/Vm
membrane permittivity	ε_m	4.4e-11 As/Vm
water relative dielectric constant	ε_w	80 As/Vm
lipid relative dielectric constant	ε_l	2 As/Vm
free diffusion coefficient	D_0	5e-10 m^2/s
Zero-field equilibrium constant	K_0	2e-2
mean average aqueous pore volume	ΔV_p	9e-27 m^3
Intrinsic barrier potential of P1 state	φ_{im1}^0	0.13 V
Intrinsic barrier potential of P2 state	φ_{im2}^0	0.084 V
A geometrical parameter	n	0.12
Decay rate coefficient for C1	k_{-1}	10^7 s^{-1}
Decay rate coefficient for P1 pores	k_{-2}	2000 s^{-1}
Decay rate coefficient for P2 pores	k_{-3}	2 s^{-1}

Table 1: Values of parameters used in simulations

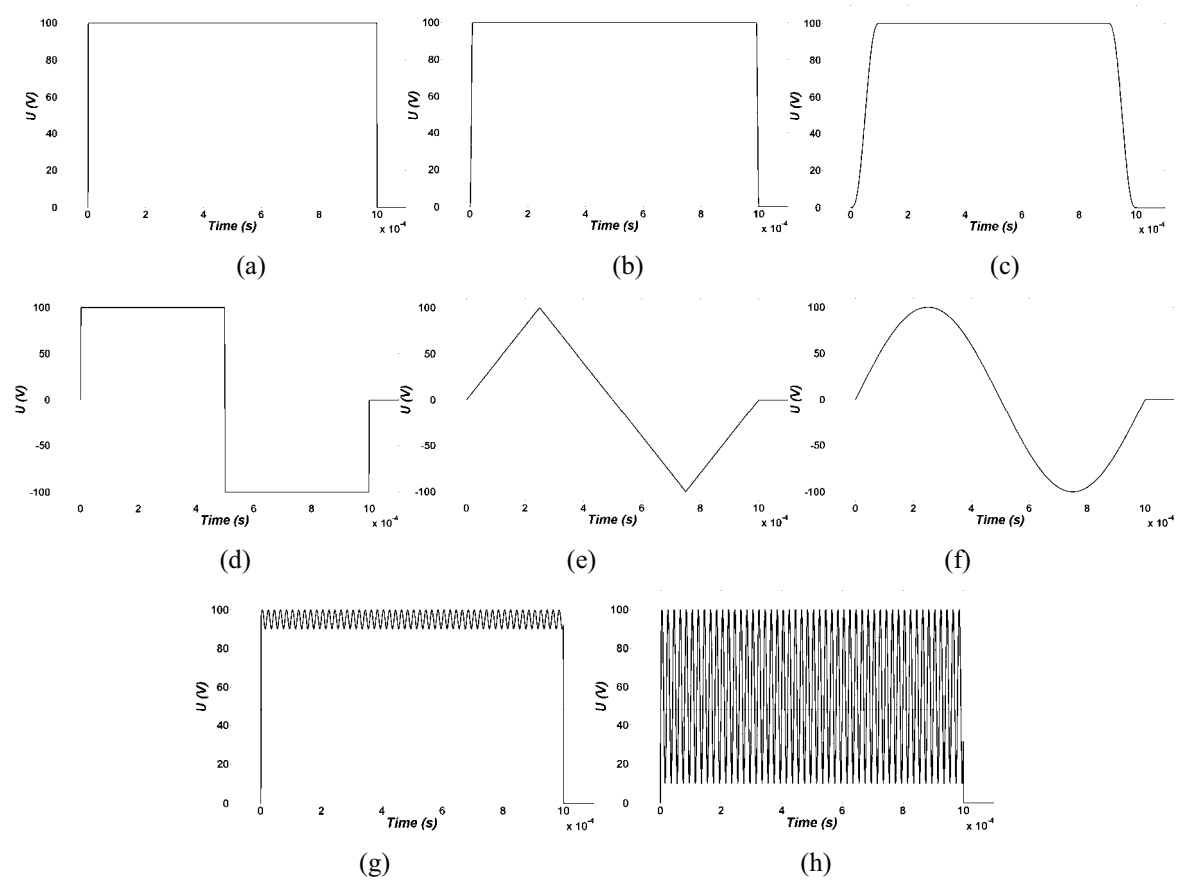

Figure 1: The investigated pulse shapes in this study. (a)-(c) are rectangular pulses with rise and fall time of 2, 10 and 100 µs, respectively. (d)-(f) are bipolar rectangular, triangular and sinusoidal pulses respectively. (g) and (f) are sine-modulated unipolar pulses with 10% and 90% modulation of 50 kHz.

4 Results

Immediately after smoothed step pulse is switched on, ITV starts to increase based on Laplace equation causes membrane structural changes initiation which in turn results in membrane conductivity increase according to Eq. (6). The temporal behavior of averaged conductivities over the cell membrane due to applying considered pulse shapes (Figures (1d) to (1h)) are shown in Figure (2). All pulses were considered to have a peak of 1 kV/cm and total duration of 1 ms.

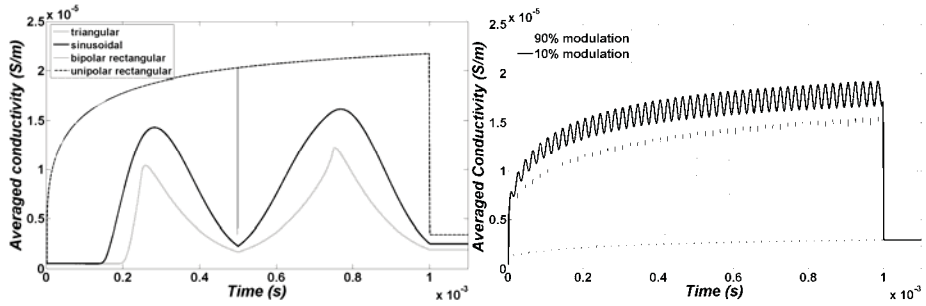

(a) (b)

Figure 2: Temporal evolution of the overall membrane conductivity during the pulse for (a) unipolar and bipolar rectangular, triangular and sinusoidal pulses and (b) 10% and 90% sine-modulated unipolar pulses.

It can be observed in the Figure (2) that the overall conductivity changes for unipolar and bipolar pulses have negligible difference. The reason for this fact is a very quick switch between positive and negative voltage and also ignoring the resting voltage in this model. Besides a comparison between conductivity increase due to rectangular, triangular and sinusoidal pulses Figure (2a) shows the most and least changes due to rectangular and triangular pulse shapes, respectively. Figure (2b) shows conductivity change due to 10% modulation is higher than 90% one but still both are lower than rectangular pulse.

The temporal behavior of averaged cell membrane permeability for pulses in Figures (1d) to (1h) is illustrated in Figure (3). Permeability changes occurs slowly, therefore for bipolar pulses and modulated pulses in which the falls and rises are very fast, there is not enough time for resealing of permeability which causes different behavior for membrane permeability related to membrane conductivity. Based on Figure (3), we expect the order of efficiency of pulses of the same peak as follows: unipolar and bipolar rectangular, 10% modulated, sine, 90% modulated and finally bipolar triangular pulses.

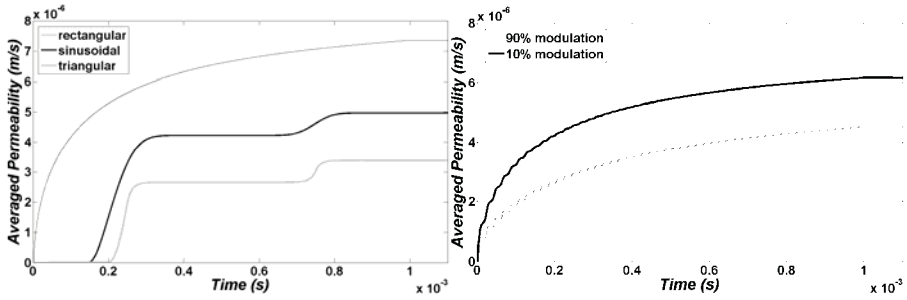

(a) (b)

Figure 3: Temporal evolution of the overall membrane permeability during the pulse for (a) unipolar and bipolar rectangular, triangular and sinusoidal pulses and (b) 10% and 90% sine-modulated unipolar pulses.

To be able to check the validity of our simulation results, the uptake enhancement of the cell were obtained for the same pulse parameters of previously obtained experimental results [11]. The chosen parameters were 8 pulses of 100 μs duration and 1 Hz pulse repetition frequency with different pulse strength for each pulse shape.

Figure (4a) shows the results of simulation for 8 pulses of bipolar rectangular, sine and triangular pulses. It shows that the rectangular pulses are more efficient than sinusoidal pulses which in turn are more efficient than triangular pulses. These results are in good agreement with experimentally obtained results [11]. The uptake due to unipolar pulses is larger than bipolar pulses but this difference is negligible (because of very fast switch between positive and negative parts) and not observable while in experimental results bipolar pulses are significantly more efficient than unipolar pulses. The reason for this inconsistency can be due to neglecting resting voltage in the simulations.

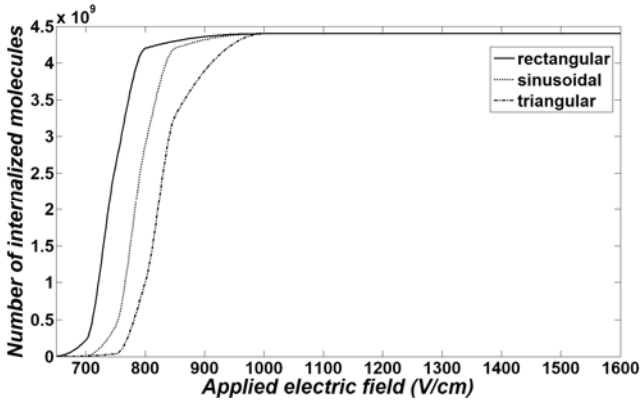

(a)

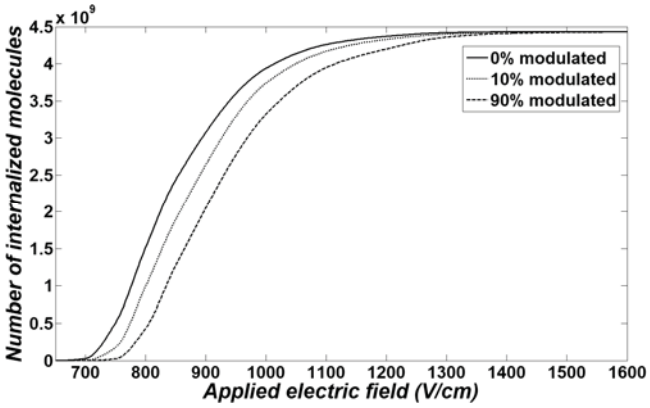

(b)

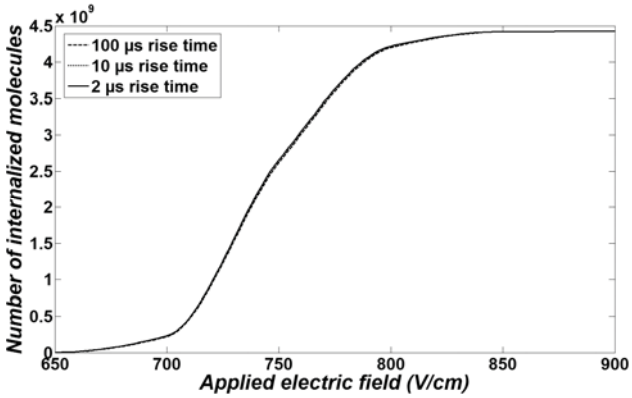

(c)

Figure 4: Dye uptake 16 minutes after pulse cessation versus electric field amplitude for (a) 8 pulses of 1 ms and 1 Hz unipolar and bipolar rectangular, triangular and sinusoidal pulses, (b) one 1 ms pulse of 0%, 10% and 90% sine-modulated and (c) 8 pulses of 1 ms rectangular pulses with rise and fall times of 2, 10 and 100 µs.

In addition, Figure (4b) demonstrates the comparison between unipolar pulses of 0, 10 and 90% modulation. The results are in good qualitative agreement with previously obtained experimental results [11]. The uptake enhancements results for 8 pulses of unipolar trapezoidal pulses of 1 ms duration with 2, 10 and 100 µs rise and fall times are shown in Figure (4c). It can be seen from figure that there is no significant difference between these pulses which is in good agreement with experimental results [11].

5 Conclusion

The described model enables determination and prediction of all electrical and diffusional parameters for different pulse shapes. Thus knowing electrical and diffusional properties of the cells and the dye, optimization of electroporation protocol can be performed. Our results show that rectangular pulses are more effective than the sinusoidal and in turn triangular pulses. Besides, the results indicated that the higher the percent of unipolar pulses modulation with sine shape pulses of 50 kHz, the lower uptake enhancement of the cells. Moreover the rise and fall times of unipolar rectangular pulses are not significantly affecting the uptake of molecules into the cells. Our simulation results are in good agreement with experimental observations.

6 References

[1] Böckmann, R. A., Groot, B. L., Kakorin, S., Neumann, E. and Grubmüller, H.: *Kinetics, Statistics, and Energetics of Lipid Membrane Electroporation Studied by Molecular Dynamics Simulations.* Biophys J, 95,4 (2008), 1837–50.

[2] DeBruin, K. A. and Krassowska,W.: *Modeling Electroporation in a Single Cell. II. Effects of Ionic Concentrations.* Biophys J, 77, 3 (1999), 1225–1233.

[3] Faurie, C., Golzio, M., Phez, E., Teissié, J. and Rols, M. P.: *Electric field induced cell membrane permeabilization and gene transfer: theory and experiments.* Eng Life Sci 5 (2005),179–186.

[4] Glogauer, M., Lee, W. and McCulloch, C. A.: *Induced endocytosis in human fibroblasts by electrical fields.* Exp Cell Res 208, 1(1993), 232–40.

[5] Golzio, M., Mazzolini, L., Moller, P., Rols, M. P. and Teissié, J.: *Inhibition of gene expression in mice muscle by in vivo electrically mediated siRNA delivery.* Gene Ther, 12 (2005), 246–251.

[6] Gowrishankar, T. R. and Weaver, J. C.: *An approach to electrical modeling of single and multiple cells.* Proc Natl Acad Sci USA, 100, 6 (2003), 3203–3208.

[7] Joshi, R. P., Hu, Q., Schoenbach, K. H. and Bebe, S. J.: *Simulations of electroporation dynamics and shape deformations in biological cells subjected to high voltage pulses.* IEEE Trans Plasma Sci, 30 (2002),1536–1546.

[8] Joshi, R. P., Hu, Q. and Schoenbach, K. H.: *Modeling studies of cell response to ultrashort, high-intensity electric fields—implications for intracellular manipulation.* IEEE Trans Plasma Sci, 32 (2004),1677–1686.

[9] Kakorin, S. and Neumann, E.: *Ionic conductivity of electroporated lipid bilayer membranes.* Bioelectrochem, 56 (2002): 163–166.

[10] Kotnik, T., Bobanovic, F. and Miklavcic, D.: *Sensitivity of transmembrane voltage induced by applied electric fields – a theoretical analysis.* Bioelectrochem Bioenerg, 43 (1997), 285–291.

[11] Kotnik, T., Pucihar, G., Rebersek, M., Mir, L. M. and Miklavcic, D.: *Role of pulse shape in cell membrane electropermeabilization.* Biochim Biophys Acta, 1614 (2003), 193-200.

[12] Mir, L. M.: *Bases and rationale of the electrochemotherapy.* Eur J Cancer Suppl, 4 (2006), 38–44.

[13] Neu, J. C. and Krassowska, W.: *Asymptotic model of electroporation.* Phys Rev E, 59 (1999), 3471–3482.

[14] Neumann, E., Schaefer-Ridder, M., Wang, Y. and Hofschneider, P. H.: *Gene transfer into mouse lyoma cells by electroporation in high electric field.* EMBO J, 1(1982):841– 845.

[15] Neumann, E., Toensing, K., Kakorin, S., Budde, P. and Frey, J.: Mechanism of electroporative dye uptake by mouse B cells. Biophys J, 74, 1 (1998), 98–108.

[16] Neumann, E., Kakorin, S. and Tönsing, K.: *Fundamentals of electroporative delivery of drugs and genes.* Bioelectrochem Bioenerg, 48 (1999), 3–16.

[17] Pavlin, M., Leben, V. and Miklavcic, D.: *Electroporation in dense cell suspension – Theoretical and experimental analysis of ion diffusion and cell permeabilization.* Biochim Biophys Acta, 1770 (2007), 12–23.

[18] Pliquett, U. and Weaver, J.C.: *Feasibility of an electrode-reservoir device for transdermal drug delivery by noninvasive skin electroporation.* IEEE Trans Biomed Eng 54, (2007), 536–538.

[19] Puc, M., Kotnik, T., Mir, L. M. and Miklavčič, D.: *Quantitative model of small molecules uptake after in vitro cell electropermeabilization.* Bioelectrochem, 60 (2003):1–10.

[20] Pucihar, G., Kotnik, T., Valic, B. and Miklavcic, D.: *Numerical determination of transmembrane voltage induced on irregularly shaped cells.* Annals Biomed Eng, 34 (2006), 642–652.

[21] Rols, M. P., Femenia, P. and Teissié, J.: *Long-lived macropinocytosis takes place in electropermeabilized mammalian cells.* Biochem Biophys Res Commun, 208 (1995), 26–38.

[22] Schmeer, M., Seipp, T., Pliquett, U., Kakorin, S. and Neumann, E.: *Mechanism for the conductivity chnages caused by membrane electroporation of CHO cell – pellets.* Phy Chem Chem Phys, 6 (2004), 5564–5574.

[23] Sersa, G., Miklavcic, D., Cemazar, M., Rudolf, Z., Pucihar, G., Snoj, M.: *Electrochemotherapy in treatment of tumours.* Eur J Surg Oncol, 34(2008), 232-40.

[24] Teissié, J. and Rols, M. P.: *An experimental evaluation of the critical potential difference inducing cell membrane electropermeabilization.* Biophys J, 65(1993), 409–413.

[25] Teissie, J., Eynard, N., Vernhes, M. C., Bénichou, A., Ganeva, V., Galutzov, B. and Cabanes, P. A.: *Recent biotechnological developments of electropulsation. A prospective review.* Bioelectrochem. 55 (2002),107–112.

[26] Zimmermann, U., Schnettler, R., Klöck, G., Watzka, H., Donath, E., Glaser, R. W.: *Mechanisms of electrostimulated uptake of macromolecules into living cells.* Naturwissenschaften, 77 (1990), 543–545.